DOI: 10.1002/chem.200700765

Site Selectivity in the Reactions of the Hexanuclear Platinum Cluster $[Pt_6(\mu\text{-}P\mathit{t}Bu_2)_4(CO)_6][CF_3SO_3]_2$

Cristina Bonaccorsi,[a] Fabrizia Fabrizi de Biani,[b] Piero Leoni,*[a] Fabio Marchetti,[a] Lorella Marchetti,[a] and Piero Zanello[b]

Abstract: The previously reported hexanuclear cluster $[Pt_6(\mu\text{-}P\mathit{t}Bu_2)_4(CO)_6]^{2+}[Y]_2$ (**1**-Y_2: $Y = CF_3SO_3^-$) contains a central Pt_4 tetrahedron bridged at each of the opposite edges by another platinum atom; in turn, four phosphido ligands bridge the four Pt–Pt bonds not involved in the tetrahedron, and, finally, one carbonyl ligand is terminally bonded to each metal centre. Interestingly, the two outer carbonyls are more easily substituted or attacked by nucleophiles than the inner four, which are bonded to the tetrahedron vertices. In fact, the reaction of **1**-Y_2 with 1 equiv of $[n\mathrm{Bu_4N}]Cl$ or with an excess of halide salts gives the monochloride $[Pt_6(\mu\text{-}P\mathit{t}Bu_2)_4(CO)_5Cl]^+[Y]$, **2**-Y, or the neutral dihalide derivatives $[Pt_6(\mu\text{-}P\mathit{t}Bu_2)_4(CO)_4X_2]$ (**3**: X = Cl; **4**: X = Br; **5**: X = I). Moreover, the useful unsymmetrically substituted $[Pt_6(\mu\text{-}P\mathit{t}Bu_2)_4(CO)_4ICl]$ (**6**) was obtained by reacting equimolar amounts of **2** and $[n\mathrm{Bu_4N}]I$, and the dicationic derivatives $[Pt_6(\mu\text{-}P\mathit{t}Bu_2)_4(CO)_4L_2]^{2+}[Y]_2$ (**7**-Y_2: $L = {}^{13}CO$; **8**-Y_2: $L = CN\mathit{t}Bu$; **9**-Y_2: $L = PMe_3$) were obtained by reaction of an excess of the ligand L with **1**-Y_2. Weaker nitrogen ligands were introduced by dissolving the dichloride **3** in acetonitrile or pyridyne in the presence of $TlPF_6$ to afford $[Pt_6(\mu\text{-}P\mathit{t}Bu_2)_4(CO)_4L_2]^{2+}[Z]_2$ ($Z = PF_6^-$, **10**-Z_2: L = MeCN; **11**-Z_2: L = Py). The "apical" carbonyls in **1**-Y_2 are also prone to nucleophilic addition (Nu^-: H^-, MeO^-) affording the acyl derivatives $[Pt_6(\mu\text{-}P\mathit{t}Bu_2)_4(CO)_4(CONu)_2]$ (**12**: Nu = H; **13**: Nu = OMe). Complex **12** is slowly converted into the dihydride $[Pt_6(\mu\text{-}P\mathit{t}Bu_2)_4(CO)_4H_2]$ (**14**), which was more cleanly prepared by reacting **3** with $NaBH_4$. In a unique case we observed a reaction involving also the inner carbonyls of complex **1**, that is, in the reaction with a large excess of the isocyanides R–NC, which form the corresponding persubstituted derivatives $[Pt_6(\mu\text{-}\mathit{t}PBu_2)_4(CN\text{–}R)_6]^{2+}[Y]_2$, (**15**-$Y_2$: R = *t*Bu; **16**-$Y_2^{2-}$: $R = -C_6H_4\text{-}4\text{-}C{\equiv}CH$). All complexes were characterized by microanalysis, IR and multinuclear NMR spectroscopy. The crystal and molecular structures of complexes **3**, **5**, **6** and **9**-Y_2 are also reported. From the redox viewpoint, all complexes display two reversible one-electron reduction steps, the location of which depends both upon the electronic effects of the substituents, and the overall charge of the original complex.

Keywords: cluster compounds · cyclic voltammetry · organometallic synthons · phosphido ligands · platinum

Introduction

The assembly of large molecular frameworks with pre-defined shape is one of the most exciting challenges for chemical research,[1] and the interest is enhanced further by possible applications in the bottom-up construction of nano-scale machines or devices.[2] The synthetic procedures employ different types of inorganic or organometallic "bricks", from simple mononuclear L_nM fragments[1–3] to dinuclear,[4] metal-chain,[5] porphyrin,[1a,6] polyoxometalate,[7] carborane,[8] C60[9] or dendrimeric[10] units, generally connected by organic bridging ligands or spacers. Owing to the peculiar redox properties of transition-metal clusters,[11] there is also a growing interest in the construction of rigid-rod or dendrimeric structures in which two[12] or more[13,14] cluster units are connected by conjugated or insulating spacers.[15] Suitable cluster building blocks should; a) be synthesizable in good yields and purity; b) be resistant to fragmentation, condensation and, possibly, also to rearrangement processes; c) contain a limited number of reactive, well positioned, sites suitable to the insertion of the spacer groups.

[a] Dr. C. Bonaccorsi, Prof. P. Leoni, Prof. F. Marchetti, Dr. L. Marchetti
Dipartimento di Chimica e Chimica Industriale
Università di Pisa, via Risorgimento, 35, 56126 Pisa (Italy)
Fax: (+39) 050-221-9260
E-mail: leoni@dcci.unipi.it

[b] Dr. F. F. de Biani, Prof. P. Zanello
Dipartimento di Chimica, Università di Siena
via A. Moro, 53100 Siena (Italy)

We have shown that the hexanuclear platinum cluster $[Pt_6(\mu\text{-}PtBu_2)_4(CO)_6]^{2+}[Y]_2$ (**1**-Y_2: $Y = CF_3SO_3^-$) which can be prepared in 3 steps and reasonable yields from commercially available reagents, has a $[Pt_6(\mu\text{-}PtBu_2)_4(CO)_4]$ core that exhibits a remarkably high thermal and chemical stability and two reactive positions, mutually directed at 180°, readily accessible for chemical transformations.[16] In this work we report the synthesis of symmetrical and unsymmetrical dihalides and other derivatives, well suited for the above cited utilization, and a thorough study on the general reactivity of complex **1**-Y_2. Part of this work has been communicated previously.[14,16] We point out that di- or polyhalo carbonyl clusters are not very common; indeed, if one excludes the slightly more numerous derivatives of the iron group, limited examples[17] (only one with a Pt containing Au_9Pt core)[17d] of such structurally characterized complexes can be found in the CCDC files.[18] To the best of our knowledge, $[Os_5PdC(CO)_{14}ICl(PPh_2Py)]$[17m] is the sole structurally characterized carbonyl cluster with two different halide ligands that has previously been reported.

Results and Discussion

Preparation of $[Pt_6(\mu\text{-}PtBu_2)_4(CO)_5Cl][Y]$ and $[Pt_6(\mu\text{-}PtBu_2)_4(CO)_4XX']$ (X = X′ = Cl, Br, I or X = I, X′ = Cl): A red CH_2Cl_2 solution of complex **1**-Y_2 was treated with an equimolar amount of $[nBu_4N]Cl$ to give, in a few minutes, the monohalide $[Pt_6(\mu\text{-}PtBu_2)_4(CO)_5Cl]^+[Y]$, **2**-Y, which was isolated in good yield (92%) as an orange microcrystalline solid (Scheme 1). The dihalides $[Pt_6(\mu\text{-}PtBu_2)_4(CO)_4X_2]$ (**3**: X = Cl; **4**: X = Br; **5**: X = I) were obtained by similar procedures employing acetone as the solvent and an excess (3- to 6-fold) of the proper halide salt (**3**, orange, 97%; **4**, orange, 91%, **5**, red, 94%). Further carbonyl substitution was not observed when reaction times and/or temperatures were increased. Finally, the unsymmetrical dihalide $[Pt_6(\mu\text{-}PtBu_2)_4(CO)_4ICl]$ (**6**) was obtained by reacting equimolar amounts of complex **2**-Y and $[nBu_4N]I$ in acetone (92%, orange). Single crystals for diffractometric studies (see below), were respectively obtained by slow evaporation of a CH_2Cl_2 solution (complex **5**), and by recrystallization from a Et_2O/acetone mixture (**3** and **6**). Significant IR and NMR parameters for complexes $\mathbf{1}^{2+}$–$\mathbf{16}^{2+}$ are shown in Table 1. Compared to its precursor $\mathbf{1}^{2+}$ ($\tilde{\nu}_{CO}$ at 2089 and 2056 cm^{-1},respectively assigned to the two apical and the four inner carbonyl ligands) the less symmetrical **2** shows, as

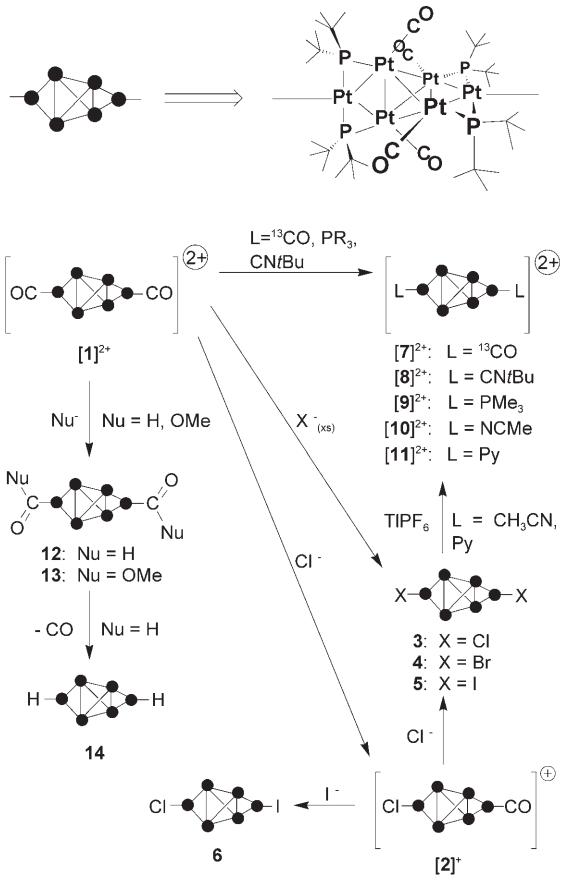

Scheme 1. General reactivity of complex **1** and of its derivatives.

Table 1. Significant IR $\tilde{\nu}$[cm^{-1}] and NMR δ[ppm] parameters for complexes $\mathbf{1}^{2+}$–$\mathbf{16}^{2+}$.[a]

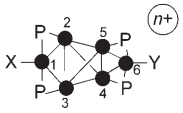

	X	Y	n	$\tilde{\nu}$[b]	$\delta_{P(1,2)}$ $\delta_{P(1,2)}$	$\delta_{Pt(1)}$ $\delta_{Pt(6)}$	$\delta_{Pt(2,3)}$ $\delta_{Pt(4,4)}$
$\mathbf{1}^{2+}$	CO	CO	2	2089, 2056	383.7	−4960	−3203
$\mathbf{2}^{+}$	CO	Cl	1	2080, 2059; 2047, 2036; 2025	360.5 348.4	−5012 −3928	−3112 −3516
3	Cl	Cl	0	2017	328.9	−4153	−3463
4	Br	Br	0	2018	330.5	−4410	−3417
5	I	I	0	2017	333.2	−4933	−3352
6	I	Cl	0	2017	333.4 328.8	−4938 −4149	−3354 −3452
$\mathbf{7}^{2+}$	^{13}CO	^{13}CO	2	2040, 2056	383.7	−4960	−3203
$\mathbf{8}^{2+}$	CN*t*Bu	CN*t*Bu	2	2046	361.6	−4954	−3182
$\mathbf{9}^{2+}$	PMe_3	PMe_3	2	2030	337.4	−5218	−2914
$\mathbf{10}^{2+}$	NCMe	NCMe	2	2023	347.9	−4417	−3525
$\mathbf{11}^{2+}$	Py	Py	2	2031	327.8	−4343	−3406
12	CHO	CHO	0	2006, 1608	316.3	−4642	−2570
13	COOMe	COOMe	0	2015, 1704	330.4	−4844	−2804
14	H	H	0	2001	342.0	−5146	−2822
$\mathbf{15}^{2+}$	CN*t*Bu	CN*t*Bu	2	2169, 2131	300.5	−5131	−3083
$\mathbf{16}^{2+}$	[c]	[c]	2	2150, 2122	323.4	−4981	−2996

[a] Each of the central Pt_{2-5} nuclei bears one terminal carbonyl ($\mathbf{1}^{2+}$–**14**) or isonitrile ($\mathbf{15}^{2+}$–$\mathbf{16}^{2+}$) ligand; [b] $\tilde{\nu}$(CO): complexes $\mathbf{1}^{2+}$–**14**; $\tilde{\nu}$(CN): complexes $\mathbf{15}^{2+}$ and $\mathbf{16}^{2+}$. [c] CN–C_6H_4–C≡CH.

expected, a more complex pattern of absorptions between $\tilde{\nu}=2080$ and 2025 cm^{-1}, while the dihalides **3–6** exhibit a unique absorption at $\approx 2017\ cm^{-1}$ for the equivalent inner carbonyls.

The shift to lower wavenumbers from **1**-Y_2 to **2**-Y, and to **3–6**, is also expected for the substitution of π-acceptor carbonyls with donor halide ligands and for charge effects. As in complex **1**-Y_2, the four P nuclei in the symmetrical dihalides **3–5** are isochronous and give, in the $^{31}P\{^1H\}$ NMR spectrum, a central singlet flanked by a complex set of ^{195}Pt satellites (owing to the superposition of the subspectra given by 64 isotopomers; ^{195}Pt, $I=1/2$, natural abundance = 33.8 %). These are very similar to the corresponding data observed for **1**-Y_2, and strong similarities were also observed in the main features of the $^{195}Pt\{^1H\}$ NMR spectrum.[19] The latter exhibits only two characteristic resonances for the apical ($Pt_{1,6}$) and inner (Pt_{2-5}) platinum nuclei, which rule out all other possible isomeric structures. The values of δ_P (383.7 ppm in **1**-Y_2) move considerably to high-field, and the shift increases slightly with increasing halide electronegativity (333.2, 330.5, and 328.9 ppm, respectively observed for **5**, **4**, and **3**), opposite to the trend generally observed in mononuclear $(R_3P)_xMX_y$ derivatives.[20] The same trend was observed for the values of $\delta_{Pt(2-5)}$ (−3203, −3352, −3417, and −3463 ppm for **1**-Y_2, **5**, **4**, and **3**), whereas the inverse drift is exhibited by the values of $\delta_{Pt(1,6)}$ (−4153, −4410, −4933, and −4960 ppm for **3**, **4**, **5**, and **1**, respectively). These intriguing trends, reasonably a result of the charge redistribution occurring upon substitution at the apical sites, cannot be straightforwardly explained, nevertheless, they are very useful for the assignment of the resonances observed for the less symmetrical **2**-Y and **6** (see Table 1). The ^1H and $^{13}C\{^1H\}$ NMR spectra of the dihalides **3–5** show the expected signals for equivalent *t*-butyl (δ_H, δ_C, and δ_{CH3} respectively at $\approx$1.5,[19] 45 and 32 ppm) and carbonyl groups (δ_C at $\approx$205 ppm); the corresponding resonances are doubled in the spectra of the asymmetrical derivatives **2**-Y and **6** (see the Experimental Section). The spectral (and microanalytical) parameters of complex **6** could also be interpreted as arising from a 1:1 mixture of **3** and **5**, however its reactivity[14c] unambiguously agrees with the given formulation.

Preparation of $[Pt_6(\mu\text{-}P\mathit{t}Bu_2)_4(CO)_4L_2][Y]_2$ (L=^{13}CO, CN*t*Bu, PMe_3) and $[Pt_6(\mu\text{-}P\mathit{t}Bu_2)_4(CO)_4L_2][Z]_2$ (L=MeCN, Py; Z=PF_6): The apical carbonyls of complex **1**-Y_2 are also selectively substituted by neutral 2 e^- donors, to give salts of the dication $[Pt_6(\mu\text{-}P\mathit{t}Bu_2)_4(CO)_4L_2]^{2+}$. Details of the reactions with ^{13}CO or PMe_3, yielding complexes **7**-Y_2 (L = ^{13}CO) or **9**-Y_2 (L = PMe_3) under mild conditions, have been given elsewhere[16] and will not be duplicated here. Single crystals of **9**-Y_2 were obtained by slow evaporation of $CHCl_3$ solutions. Complex **1**-Y_2 reacts at room temperature with 2 equiv of *t*-butylisocyanide to give **8**-Y_2 (L = CN*t*Bu) as a red solid (86 %). Complexes of weaker ligands were obtained under stronger conditions starting from the dichloride **3**, which must be warmed at 60 °C for 12 H, in acetonitrile or pyridine solution and in the presence of $TlPF_6$, to give the corresponding disubstituted derivatives **10**-Z_2 (L = MeCN, Z = PF_6, 78 %) and **11**-Z_2 (L = Py, 71 %) as analytically pure orange solids. The presence of the Pt-bonded nitrogen ligands was certified by the resonances at δ_H = 2.93 ppm (s, with satellites, $^4J_{HPt}=10.6$ Hz, 3H; CH_3CN), $\delta_C=4.30$ ppm (CH_3CN) and by the IR absorption $\tilde{\nu}_{CN}$ = 2309 cm^{-1} for **10**-Z_2 and by the resonances at $\delta_H=9.5$ (d, $^3J_{HH}=5.0$ Hz, with satellites, $^3J_{HPt}=45$ Hz, 4H), 8.3 (t, $^3J_{HH}$ = 7.5 Hz, 2H), 8.0 ppm (dt, $^3J_{HH}=7.5$, 5.0 Hz, 4H) and δ_C = 156.2, 141.8 and 129.3 ppm for **11**-Z_2. The remaining signals in the ^1H and $^{13}C\{^1H\}$ NMR and the $^{31}P\{^1H\}$ and $^{195}Pt\{^1H\}$ NMR spectra (Table 1) fulfilled expected shape and position expectations.

Preparation of $[Pt_6(\mu\text{-}P\mathit{t}Bu_2)_4(CO)_4(CONu)_2]$ (Nu = H, OMe) and $[Pt_6(\mu\text{-}P\mathit{t}Bu_2)_4(CO)_4H_2]$: Nucleophilic attacks to the carbonyl ligands are again selectively directed towards the apical positions. As detailed previously,[16] the reaction of complex **1**-Y_2 with $NaBH_4$ yields the first platinum formyl $[Pt_6(\mu\text{-}P\mathit{t}Bu_2)_4(CO)_4(CHO)_2]$, (**12**), which decarbonylates slowly to give $[Pt_6(\mu\text{-}P\mathit{t}Bu_2)_4(CO)_4H_2]$, (**14**), as the main product. The dihydride **14** can also be prepared in better yields (84 %) and purity by reacting the dichloride **3** with $NaBH_4$ (see Experimental Section). The reaction of **1**-Y_2 with $LiOCH_3$ gives $[Pt_6(\mu\text{-}P\mathit{t}Bu_2)_4(CO)_4(COOCH_3)_2]$ (**13**), as a thermally stable orange solid (84 %). Significant spectroscopic parameters for **13**, not reported in Table 1, are at $\delta_H=3.62$ ppm (s, 3H; OCH_3) and at $\tilde{\nu}_{CO}$ = 2015 (s) and 1704 cm^{-1} (m).

Preparation of $[Pt_6(\mu\text{-}P\mathit{t}Bu_2)_4(CN{-}R)_6][Y]_2$: The four carbonyls bonded to the inner tetrahedron, which are left unchanged in the reactions shown above, were indeed easily substituted when complex **1**-Y_2 was reacted with a large excess ($\approx$1:20) of isocyanide donors. The reactions occur under mild conditions, affording the per-substituted derivatives $[Pt_6(\mu\text{-}P\mathit{t}Bu_2)_4(CN{-}R)_6][Y]_2$, (**15**-$Y_2$: R = *t*Bu; **16**-$Y_2$: R = $-C_6H_4$-4-C≡CH), which were isolated as red powders in good yields (≥75 %). The new complexes retain the main structural features of complex **1**-Y_2, as inferred by the shape and the position of the $^{31}P\{^1H\}$ and $^{195}Pt\{^1H\}$ NMR resonances (Table 1). The ^1H, $^{13}C\{^1H\}$ NMR and IR spectra confirm the absence of the carbonyl ligands, the presence of two different types of isocyanide ligands, and the expected integral ratio between R_{apical}, $R_{internal}$, and the *t*-butyl groups (see Experimental Section).

Crystal and Molecular Structures: Single crystals of **3**, **5**, **6**, and **9**-Y_2 were grown as detailed above. Selected bond distances and angles are reported in Table 2 (**3**, **5**, **6**) and in Table 3 (**9**-Y_2); ORTEP projections of the molecular structures are shown in Figures 1, 2, and 3.

The structures retain the main features that we have already observed in the structurally related **1**-Y_2,[16] $[\{Pt_6\}(C{\equiv}C{-}Ph)_2]$,[14b] $[\{Pt_6\}(C{\equiv}C{-}Fc)_2]$ (Fc = $\{(\eta^5\text{-}C_5H_5)Fe(\eta^5\text{-}C_5H_4)\}$)[14d] and $[(Pt_6)(C{\equiv}C{-}C_6H_3{-}[C{\equiv}C{-}\{Pt_3\}]_2)_2]$ ($\{Pt_3\}$ = $\{Pt_3(P\mathit{t}Bu_2)_3(CO)_2\}$),[14a] that are otherwise exceedingly rare

Table 2. Selected bond lengths [Å] and angles [°] in the isotypic structures of compounds **3**, **5** and **6**. The apexes in the atom labels have the meaning shown in Figure 1.

	3	**5**	**6**
Pt(1)−Pt(2)	2.6921(3)	2.709(1)	2.696(1)
Pt(1)−Pt(1′)	2.6916(3)	2.685(1)	2.695(1)
Pt(1)−Pt(1″)	2.8674(3)	2.872(1)	2.869(1)
Pt(2)−I	–	2.643(2)	2.721(4)
Pt(2)−Cl	2.344(2)	–	2.28(1)
Pt(2)−P	2.2797(12)	2.277(4)	2.281(4)
Pt(1)−P	2.2496(11)	2.245(4)	2.246(4)
Pt(1)−C(1)	1.857(5)	1.87(2)	1.83(2)
Pt(1)-Pt(2)-Pt(1′)	59.988(9)	59.42(3)	59.97(3)
Pt(2)-Pt(1)-Pt(1′)	60.006(4)	60.29(2)	60.01(2)
Pt(1′)-Pt(1)-Pt(1″)	62.009(3)	62.13(1)	61.99(1)
Pt(1″)-Pt(1)-Pt(1‴)	55.983(7)	55.75(3)	56.02(2)

Table 3. Selected bond lengths [Å] and angles [°] in the structure of **9**-Y_2·$CHCl_3$.

Pt(1)−Pt(2)	2.799(1)	Pt(1)−Pt(3)	2.612(1)
Pt(1)−Pt(4)	2.834(1)	Pt(1)−Pt(6)	2.856(1)
Pt(2)−Pt(3)	2.808(1)	Pt(3)−Pt(4)	2.849(1)
Pt(3)−Pt(6)	2.858(1)	Pt(4)−Pt(5)	2.788(1)
Pt(4)−Pt(6)	2.615(1)	Pt(5)−Pt(6)	2.801(1)
Pt(1)−P(1)	2.251(4)	Pt(2)−P(1)	2.288(4)
Pt(2)−P(2)	2.306(4)	Pt(2)−P(3)	2.315(4)
Pt(3)−P(3)	2.269(4)	Pt(4)−P(4)	2.242(4)
Pt(5)−P(4)	2.301(4)	Pt(5)−P(5)	2.287(4)
Pt(5)−P(6)	2.303(4)	Pt(6)−P(6)	2.264(4)
Pt(1)−C(1)	1.92(2)	Pt(3)−(2)	1.86(2)
Pt(4)−C(3)	1.82(2)	Pt(6)−C(4)	1.92(2)
Pt(1)-Pt(2)-Pt(3)	55.53(2)	Pt(2)-Pt(1)-Pt(3)	62.40(2)
Pt(1)-Pt(3)-Pt(2)	62.07(2)	Pt(3)-Pt(1)-Pt(4)	62.93(2)
Pt(3)-Pt(1)-Pt(6)	62.85(2)	Pt(4)-Pt(1)-Pt(6)	54.74(2)
Pt(1)-Pt(3)-Pt(4)	62.34(2)	Pt(1)-Pt(3)-Pt(6)	62.75(2)
Pt(4)-Pt(3)-Pt(6)	54.55(2)	Pt(1)-Pt(6)-Pt(3)	54.41(2)
Pt(1)-Pt(6)-Pt(4)	62.21(2)	Pt(3)-Pt(6)-Pt(4)	62.54(2)
Pt(1)-Pt(4)-Pt(3)	54.73(2)	Pt(1)-Pt(4)-Pt(6)	63.06(2)
Pt(3)-Pt(4)-Pt(6)	62.91(2)	Pt(5)-Pt(4)-Pt(6)	62.36(2)
Pt(4)-Pt(6)-Pt(5)	61.84(2)	Pt(4)-Pt(5)-Pt(6)	55.80(2)

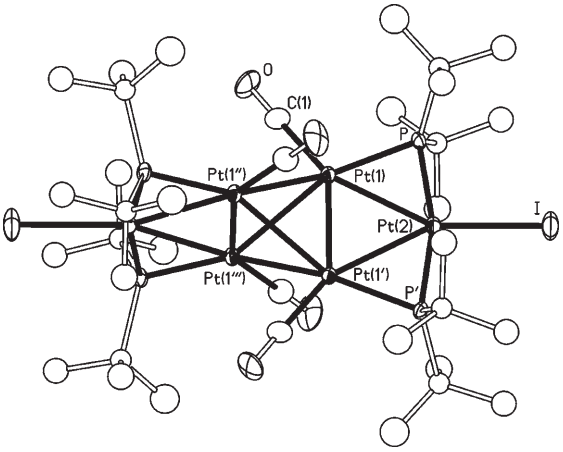

Figure 1. View of the molecular structure of $[Pt_6(\mu\text{-}PtBu_2)_4(CO)_4I_2]$, **5**. Ellipsoids are at 30% probability. Hydrogen atoms have been removed and only the most populated positions of the disordered methyl groups have been represented for sake of clarity. $'=1-x, {}^1/_2-y, z$; $''=1/4+y, 3/4-x, 1/4-z$; $'''=3/4-y, -1/4+x, 1/4-z$.

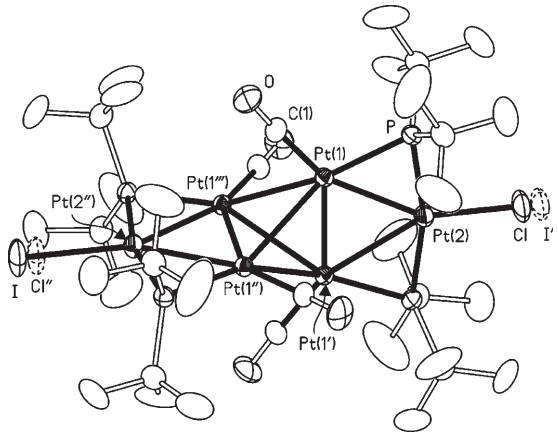

Figure 2. View of the molecular structure of $[Pt_6(\mu\text{-}PtBu_2)_4(CO)_4ICl]$, **6**. Ellipsoids are at 30% probability. Hydrogen atoms have been removed for clarity. The apexes in the labels have the same meaning as in Figure 1. The dashed ellipsoids remark the orientational disorder of the molecules in the crystal.

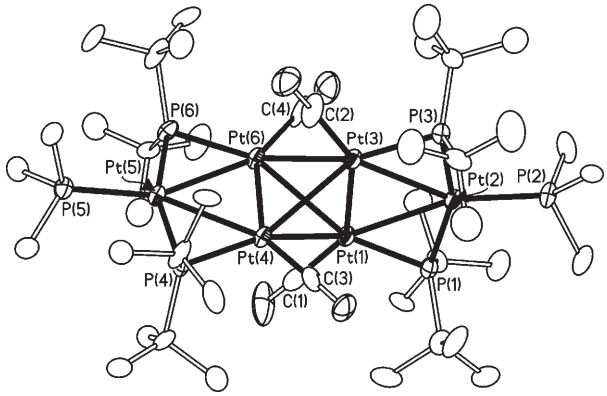

Figure 3. View of the molecular structure of the cation $[Pt_6(\mu\text{-}PtBu_2)_4(CO)_4(PMe_3)_2]^{2+}$ as it appears in the structure of **9**-Y_2·$CHCl_3$. Ellipsoids are at 30% probability. Hydrogen atoms have been removed for clarity.

for hexanuclear complexes of the whole transition series. All these complexes contain a tetrahedral core of platinum atoms with two opposite edges bridged by a further two ("apical") platinum centers. Each of the four external Pt−Pt bonds of the dibridged tetrahedron (dbt) is bridged by one bulky $PtBu_2$ phosphido ligand, while the four inner edges of the tetrahedron are unbridged. One terminally bonded carbonyl ligand on each of the central Pt_4 centers completes the structure of the $\{Pt_6\}$ core.

The overall structures show a D_{2d} local symmetry, with the variable XY ligands bonded to the apical platinum centers nearly aligned with the major S_4 axis. The monoclinic **9**-Y_2 deviates only slightly from this symmetry. The central $\{Pt_6\}$ skeleton, common to all of these complexes, is only slightly stretched upon substitution of the XY ligands; indeed, the stretching is significant for only the external triangles and less so for the inner Pt−Pt bonds. Bond a (Scheme 2) are constantly lengthened from 2.696(1) to 2.801(1) Å in the series XY = halides, alkynyls, CO, PMe_3,

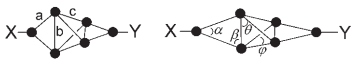

Scheme 2. Stretching of the $\{Pt_6\}$ core upon substitution of X, Y ligands.

while Pt–Pt bonds b (Scheme 2) are shortened from 2.695(1) to 2.612(1) Å; outer bonds c (Scheme 2) remain in the shorter range from 2.834(1) to 2.872(1) Å. Bond angles are modified accordingly, with the most relevant variations observed for angles α, which decrease from 59.97(3) to 55.53(2)°, in the same series.

The Pt–Pt, Pt–P and Pt–CO bond distances in **3**, **5**, **6** and **9**-Y_2 fall in the range normally found in this type of clusters, while the Pt–halogen distances deserve some comment. In fact, clusters of Groups 9 and 10 with halide ligands are relatively rare, moreover, in the few known examples, bridging μ_2- or μ_3-X coordination is preferred,[21] unless other strongly bridging groups such as μ-E (E = S, Se, P, As) or μ-ER (E = N, P) are present.[22] As a consequence, clusters of these groups with terminally bonded halides are exceedingly rare. For example, as far as we know there is only a previous example of Pt cluster with a terminal chloride, $[Pt_3(\mu_3\text{-}CO)(\mu_2\text{-}dppm)_3Cl][Cl]$,[23a] in which the chloride ligand is very weakly bonded perpendicularly to the Pt_3 triangle and exhibits a long Pt–Cl distance (2.784 Å). Those found in **3** and **6**, where the Pt–Cl bond is parallel to the adjacent Pt_3 triangle, are much shorter (2.344(2) and 2.28(1) Å, respectively) but are, on the other hand, in the range observed for Pt–Cl bond lengths in linear polynuclear derivatives (2.280–2.498 Å).[23b–e]

The Pt–I bond distances exhibited by **5** (2.643(3) Å) and **6** (2.721(4) Å) are comparable to those observed in the only four platinum clusters with terminal iodide ligands reported so far: $[Pt_3(\mu_2\text{-}CO)_3I(CH_2CN)(PCy_3)_3]$ (2.729(1) Å), $[Pt_3(\mu_2\text{-}CO)_2(\mu_2\text{-}I)I(PCy_3)_3]$ (2.7524(11) Å),[24a] $[Pt_3(\mu_2\text{-}CO)_2(\mu_2\text{-}PPh_2)I(PPh_3)_3]$ (2.8165(17) Å),[24b] and $[Pt_4(\mu_2\text{-}PPh_2CH_2PPh_2)_2(\mu_2\text{-}PPh_2)_2I_2]$ (2.664(1) Å).[24c] It is also worth noting that, as compared to the corresponding distances in **3** and **5**, complex **6** exhibits a shorter Pt–Cl (2.28(1) vs. 2.344(2) Å) and a longer Pt–I bond (2.721(4) vs. 2.643(3) Å).

All molecules crystallize in the tetragonal system, with their 4-(S_4) axis, passing through the halogen atoms, parallel to *c*, along which they are perfectly aligned and eclipsed (Figure 4A).

Interestingly, the strictly linear columns formed, are arranged in an ordered 3-D array with tiny channels running along *c*, probably a result of the roughly tetrahedral (Figure 4B,C) van der Waals molecular shape of **3**–**5** and **6**, given by the *t*-butylphosphido groups, which bridge the mutually perpendicular triangles. Despite the great similarity in composition and shape, **3**, **5**, and **6** adopt different space groups, namely $I\bar{4}2d$ (**3**) and $I4_1/amd$ (**5**, **6**). The mirror planes parallel to *ab* and to *ac*, exhibited by the structures of **5** and **6**, are lacking in **3**, in which the adjacent columns are rotated by about 5° clockwise and anticlockwise, as shown in Figure 4D. As a consequence, the section of the hydrophobic

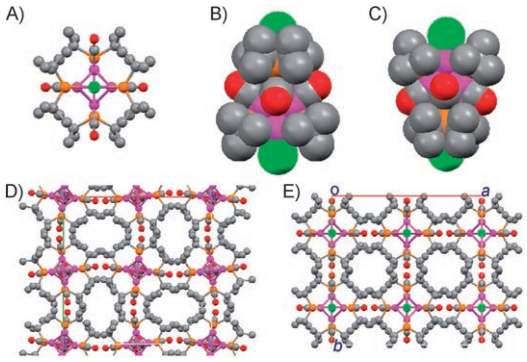

Figure 4. View of the molecular shape and packing of **3**, **5** and **6**. Hydrogen atoms have been omitted for clarity. A) A row of molecules of **5** projected along the S_4 axis. B) and C) A molecule of **5** in a space-filling representation viewed in the *a* and *b* axis directions. D) Crystal packing of **3** in the *c* direction. E) Crystal packing of **5** and **6** in the *c* direction (grey: carbon; orange: phosphorus; red: oxygen; violet: platinum; green: iodine).

channels, formed by the *t*-butyl groups, is elliptical in the structure of **3** and roughly circular in that of **5** and **6**.

Although aesthetically appealing the channels are too narrow to host incoming small molecules, however, there is more room along the chains. Indeed, in the *c* direction, the molecules of each row are not in close contact, but are spaced by holes; for example the Cl···Cl distance between chlorine atoms of adjacent molecules in **3** is 6.173 Å (Figure 5), and the corresponding Pt···Pt distance is nearly constant across the series (10.861, 10.837, 11.073 Å in **3**, **5** and **6**, respectively). This suggests that a careful selection of spacers with the proper length (and small steric encumbrance) may allow the synthesis of linear polymers that exhibit a similar solid state packing.

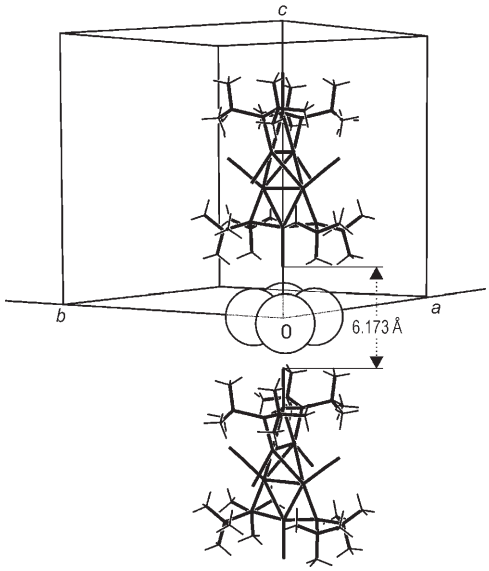

Figure 5. Section of a molecular row in the crystal structures of **3**. One of the spacing holes with four-lobes shape is also shown.

Electrochemical Study: As previously reported,[25] a CH_2Cl_2 solution of **1** exhibits two separate one-electron reductions (−0.27 and −0.54 V, vs. SCE) that possess features of chemical reversibility in the cyclic voltammetric time scale, followed by a further, partially chemically reversible, two-electron reduction at more negative potential values (−1.72 V).[26] All the halide derivatives arising from cation $\mathbf{1}^{2+}$ exhibit an expectedly large cathodic shift of all the redox processes, so that only the two first reductions become detectable (at −0.84 and −1.14 V for cation $\mathbf{2}^{+}$, and ≈ -1.4 and ≈ -1.6 V for **3**–**6**) and an irreversible oxidation process (a two-electron step based on the relative peak heights) appears at +1.2 and 1.6 V. Representatively, Figure 6 compares the CV profile of $\mathbf{1}^{2+}$ with those of $\mathbf{2}^{+}$ and **3** (profiles given by **4**–**6** are very similar to the one shown for **3**); the formal electrode potentials are compiled in Table 4.

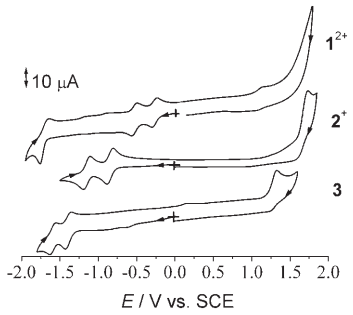

Figure 6. Cyclic voltammograms recorded at a platinum electrode in CH_2Cl_2 solution of **1** (0.6×10^{-3} mol dm^{-3}), **2** (0.7×10^{-3} mol dm^{-3}) and **3** (0.6×10^{-3} mol dm^{-3}), respectively. $[NBu_4][PF_6]$ (0.2 mol dm^{-3}) as the supporting electrolyte. Scan rate 0.2 V s^{-1}.

Table 4. Formal electrode potentials (V, vs. SCE) and peak-to-peak separations (mV) for the redox changes exhibited by cation $\mathbf{1}^{2+}$ and its derivatives in CH_2Cl_2 solution.

	Reduction processes				Oxidation process	
	$E^{0\prime}$	ΔE_p [a]	$E^{0\prime}$	ΔE_p [a]	$E^{0\prime}$	ΔE_p [a]
$\mathbf{1}^{2+}$	−0.27	58	−0.54	60	–	–
$\mathbf{2}^{+}$	−0.84	78	−1.14	82	+1.65[b,a]	–
3	−1.38	60	−1.60	94	+1.30[b,a]	–
4	−1.38	70	−1.60	70	+1.30[b,a]	–
5	−1.40	76	−1.60	78	+1.20	100
6	−1.44	72	−1.64	72	+1.20[b,a]	–
$\mathbf{8}^{2+}$	−0.71	80	−0.99	96	–	–
$\mathbf{15}^{2+}$	−1.45	78	−1.74	82	+0.88	75

[a] Measured at 0.1 V s^{-1}; [b] peak potential value for irreversible processes.

The first couple of reductions of $\mathbf{2}^{+}$ and **3**, with scan rates progressively increasing from 0.02 to 1.00 V s^{-1}, confirms their chemically and electrochemically reversible one-electron nature:1) The current ratio (i_{pa}/i_{pc}) is constantly equal to 1.0, 2) the current function, $i_{pc}\,\nu^{-1/2}$, remains substantially constant, and 3) the peak-to-peak separation, ΔE_p, approaches the theoretical value of 59 mV.[27]

As shown in Figure 7, the substitution of the two apical carbonyls of $\mathbf{1}^{2+}$ with CN*t*Bu, yielding the dication $\mathbf{8}^{2+}$, causes a considerable shift toward negative potential values (−0.71 and −0.99 V) of the two reversible steps.

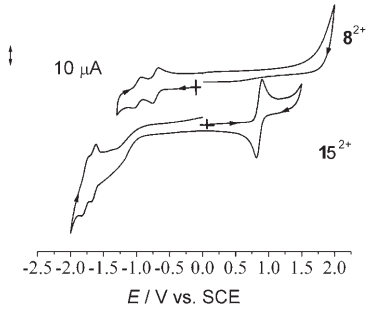

Figure 7. Cyclic voltammograms recorded at a platinum electrode in CH_2Cl_2 solution of **8** (0.6×10^{-3} mol dm^{-3}) and **15** (0.6×10^{-3} mol dm^{-3}), respectively. $[NBu_4][PF_6]$ (0.2 mol dm^{-3}) as the supporting electrolyte. Scan rate 0.2 V s^{-1}.

Figure 7 shows also that for cation $\mathbf{15}^{2+}$ in which *all* the carbonyl ligands have been substituted by CN*t*Bu, the corresponding potentials are further cathodically shifted to values (−1.45 and −1.75 V) lower than those of the neutral dihalides **3**–**6**. As a consequence of such shift, a chemically reversible oxidation, which has been confidently assumed as a two-electron process, also appears at +0.88 V.

For sake of simplicity, the discussion about the electronic effects on the redox potentials of the different complexes will be limited to the two sequential one-electron reductions, which substantially typify the redox fingerprint of our clusters.

The simple comparison of the redox potentials of $\mathbf{2}^{+}$ and **3** indicates that the progressive substitution of the apical carbonyl groups by chloride ion progressively shifts towards more negative potential values the reduction processes (by 0.6 V and 1.1 V, respectively).

The effect must certainly be ascribed either to the presence of the σ-donor chloride ligand in place of a π-acid carbonyl, or to the coulombic effects exerted by the decrease of the overall positive charge. In fact, such a trend is in agreement with the red shift of the stretching frequencies of the equivalent inner carbonyls on passing from $\mathbf{1}^{2+}$ to $\mathbf{2}^{+}$ and to **3**–**6**, a behavior which is usually attributed to charge effects (a linear correlation holds between the total charge of the clusters and the $\tilde{\nu}_{CO}$ frequencies of the four inner carbonyls, except for the mismatch of complex $\mathbf{8}^{2+}$). On the other hand, the notably different redox potentials of the isocharged cations $\mathbf{1}^{2+}$, $\mathbf{8}^{2+}$, $\mathbf{15}^{2+}$ undoubtedly prove that ligand inductive effects also play a determinant role.

The averaged position of the potential values of the asymmetric species $\mathbf{2}^{+}$ as compared to those of $\mathbf{1}^{2+}$ and **3**, together with the evidence that, independently from the apical or core position of the isonitrile ligands, their electron-donating effects are merely additive (−0.22 V/CN*t*Bu), suggests a substantial delocalization along the whole of their hexanuclear

structures. The alternative view of the structures, based on the central Pt_4 tetrahedron bridged through the phosphides by two apical, not mutually communicating, Pt atoms, does not fit the above set of experimental data.

In further accord with a significant delocalization within the Pt_6 framework, a linear relationship between the $\tilde{\nu}_{CO}$ frequencies of the four inner carbonyls and the redox potentials of the different complexes is expected and found, Figure 8.

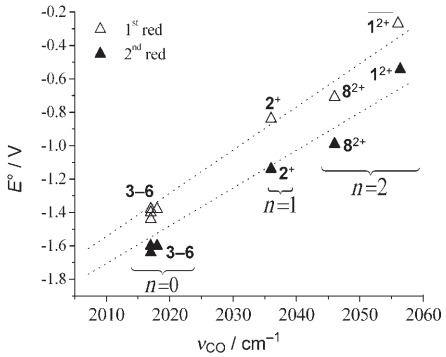

Figure 8. Relationships between the experimental CO stretching frequencies and redox potential values for the derivatives under study. The charge of the different compounds is indicated by *n* in the graph. Dashed lines show the best fits.

Noteworthy, in this case cation $\mathbf{8}^{2+}$ also fits the linear trend, further validating the influence of both the charge and the nature of the apical ligands on the electron transfer activity of the present complexes. The chance to functionalize, in different conditions, the apical or core position of the clusters and their delocalized character, is very appealing for the use of these systems as cluster building blocks for extended structures. In this respect, learning to modulate the electronic communications between the apical positions, that is, to find the conditions in which the central tetrahedral core toggles between a connecting and an insulating behavior, would be a further important challenge.

Experimental Section

General Data: The reactions were carried out under a nitrogen atmosphere, by using standard Schlenk techniques. Complexes **1**-Y_2,[16,25] **2**-Y,[25] **3**,[14a] **6**,[14c] and **9**-Y_2[16] were prepared as previously described. Solvents were dried by conventional methods and distilled under a nitrogen atmosphere prior to use. IR spectra (nujol mulls, KBr) were recorded on a Perkin–Elmer FT-IR 1725X spectrophotometer. NMR spectra were recorded on a Varian Gemini 200 BB instrument; frequencies are referenced to the residual resonances of the deuterated solvent (H, ^{13}C), 85% H_3PO_4 (^{31}P) and H_2PtCl_6 (^{195}Pt). Electrochemical measurements were performed in a dichloromethane solution that contained [N*t*Bu$_4$][PF_6] (0.2 mol dm^{-3}) as the supporting electrolyte. Anhydrous 99.9% dichloromethane was obtained from Aldrich. Electrochemical grade [N*t*Bu$_4$][PF_6] was purchased from Fluka and used as obtained. Cyclic voltammetry was performed in a three-electrode cell containing a platinum working electrode surrounded by a platinum-spiral counter electrode, and an aqueous saturated calomel reference electrode (SCE) mounted with a Luggin capillary. A BAS 100W electrochemical analyzer was used as polarizing unit. All the potential values are referred to the SCE. Under the present experimental conditions, the one-electron oxidation of ferrocene occurs at $E^0 = +0.39$ V. Controlled potential coulometry was performed in an H-shaped cell with anodic and cathodic compartments separated by a sintered-glass disk. The working macroelectrode was a platinum gauze; a mercury pool was used as the counter electrode.

Preparation of [Pt_6(μ-P*t*Bu$_2$)$_4$(CO)$_4$Br$_2$] (4): A solution of NH_4Br (75 μL, 0.075 mmol, 1 M) in acetone was added to a red colored solution of acetone (3 mL) and complex **1** (30 mg, 0.013 mmol). An orange solid precipitated out within a few minutes and was then filtered and consequently dried in vacuo (25 mg, 91%). ^1H NMR ($CDCl_3$, 25°C) $\delta =$ 1.50 ppm (vt, $^3J_{HP} + {}^5J_{HP} = 7.5$ Hz); $^{13}C\{^1H\}$ NMR ($CDCl_3$, 25°C): $\delta = 205.2$ (s, *C*O), 45.2 (P*C*), 32.1 ppm (*C*H$_3$); $^{31}P\{^1H\}$ NMR ([D$_8$]thf, 25°C): $\delta = 330.5$ ppm (s); $^{195}Pt\{^1H\}$ NMR ($CDCl_3$, 25°C): $\delta = -4410$ (2Pt), −3417 ppm (4Pt); IR (CH_2Cl_2): $\tilde{\nu}_{CO} = 2018$ cm^{-1}; elemental analysis calcd (%) for $C_{36}H_{72}Br_2O_4P_4Pt_6$: C 21.4, H 3.59; found: C 21.6, H 3.47.

Preparation of [Pt_6(μ-P*t*Bu$_2$)$_4$(CO)$_4$I$_2$] (5): KI (18 mg, 0.11 mmol) was added to a red colored solution of acetone (3 mL) and complex **1** (40 mg, 0.018 mmol). An red solid precipitated out within a few minutes and was then filtered and consequently dried in vacuo (36 mg, 94%). ^1H NMR (CD_2Cl_2, 25°C) $\delta = 1.50$ ppm (vt, $^3J_{HP} + {}^5J_{HP} = 7.4$ Hz); $^{13}C\{^1H\}$ NMR (CD_2Cl_2, 25°C): $\delta = 206.1$ (s, *C*O), 45.4 (P*C*), 32.5 ppm (*C*H$_3$); $^{31}P\{^1H\}$ NMR ([D$_8$]thf, 25°C): $\delta = 333.2$ ppm (s); $^{195}Pt\{^1H\}$ NMR (CD_2Cl_2, 25°C): $\delta = -4933$ (2Pt), −3352 ppm (4Pt); IR (CH_2Cl_2): $\tilde{\nu} = 2017$ cm^{-1} (CO); elemental analysis calcd (%) for $C_{36}H_{72}I_2O_4P_4Pt_6$: C 20.4, H 3.43; found: C 20.1, H 3.19.

Preparation of [Pt_6(μ-P*t*Bu$_2$)$_4$(CO)$_4$(CN*t*Bu)$_2$][CF_3SO_3]$_2$ (8-Y$_2$): *t*-Butylisocyanide (6 μL, $d = 0.735$ g mL^{-1}; 0.053 mmol) was added to a red colored solution of acetone (5 mL) and complex **1**-Y_2 (51 mg, 0.023 mmol). The solution quickly turned deep red and, after a few minutes, the solvent was evaporated and the residue suspended in Et_2O (10 mL). A red powder was isolated by filtration and vacuum dried (46 mg, 86%). ^1H NMR ([D$_6$]acetone, 25°C) $\delta = 1.68$ (s, 18H; NCC*H*$_3$), 1.47 ppm (vt, ^3J(H,P) + ^5J(H,P) = 8 Hz, 72H; PCC*H*$_3$); $^{13}C\{^1H\}$ NMR ($CDCl_3$, 25°C): $\delta =$ 208.0 (s, CO), 61.6 (s, CN*C*), 45.9 (s, P*C*), 31.6 (s, *C*H$_3$), 29.8 ppm (s, CNC*C*H$_3$); ^{31}P NMR ([D$_6$]acetone, 25°C) $\delta = 361.6$ ppm (s); $^{195}Pt\{^1H\}$ NMR ($CDCl_3$, 25°C): $\delta = -4954$ (m, 2Pt), −3182 ppm (m, 4Pt); IR (CH_2Cl_2): $\tilde{\nu} = 2170$ (CO), 2046 cm^{-1} (CO); elemental analysis calcd (%) for $C_{48}H_{90}F_6N_2O_{10}P_4Pt_6S_2$: C 24.8, H 3.90, N 1.20; found: C 25.0, H 3.78, N 1.22.

Preparation of [Pt_6(μ-P*t*Bu$_2$)$_4$(CO)$_4$(NC−CH$_3$)$_2$][PF_6]$_2$ (10-Z$_2$): $TlPF_6$ (40 mg, 0.11 mmol) and complex **3** (99 mg, 0.051 mmol) were suspended in CH_3CN (5 mL) and stirred for 12 h at 60°C. TlCl was filtered off and the remaining orange solution was concentrated. The addition of THF caused the precipitation of an orange powder, which was isolated by filtration and vacuum dried (89 mg, 78%). ^1H NMR ([D$_6$]acetone, 25°C) $\delta =$ 2.93 (s, $^4J_{HPt} = 10.6$ Hz, 6H; NCC*H*$_3$), 1.55 ppm (vt, ^3J(H,P) + ^5J(H,P) = 7.9 Hz, 72H; PCC*H*$_3$); $^{13}C\{^1H\}$ NMR ([D$_6$]acetone, 25°C): $\delta =$ 46.2 (P*C*), 31.6 (PC*C*H$_3$), 4.3 ppm (*C*H$_3$CN); ^{31}P NMR ([D$_6$]acetone, 25°C) $\delta = 347.9$ (s), −137.2 ppm (sept, $^1J_{PF} = 708$ Hz, PF_6); $^{195}Pt\{^1H\}$ NMR ([D$_6$]acetone, 25°C): $\delta = -4417$ (2Pt), −3525 ppm (4Pt). IR (KBr, nujol): $\tilde{\nu} = 2309$ (CN), 2023 cm^{-1} (CO); elemental analysis calcd (%) for $C_{40}H_{78}F_{12}N_2O_4P_6Pt_6$: C 21.5, H 3.52; found: C 21.2, H 3.34.

Preparation of [Pt_6(μ-P*t*Bu$_2$)$_4$(CO)$_4$(Py)$_2$][PF_6]$_2$ (11-Z$_2$): $TlPF_6$ (12 mg, 0.03 mmol) was added to a solution of pyridine (3 mL) and complex **3** (20 mg, 0.01 mmol). The resultant solution was stirred for 12 h at 60°C. TlCl precipitated out slowly and was filtered off. After the addition of Et_2O to the orange solution, complex **11**-Z_2 precipitated out as an orange powder and isolated by filtration and vacuum dried (17 mg, 71%). ^1H NMR ([D$_6$]acetone, 25°C) $\delta = 9.5$ (d, $^3J_{HH} = 5.0$, $^3J_{HPt} = 45$ Hz, 4H; Py), 8.3 (d, $^3J_{HH} = 7.5$ Hz, 2H; Py), 8.0 (dt, $^3J_{HH} = 7.5$, 5.0 Hz, 4H; Py),1.47 ppm (vt, ^3J(H,P) + ^5J(H,P) = 7.6 Hz, 72H; PCC*H*$_3$); $^{13}C\{^1H\}$ NMR ([D$_6$]acetone, 25°C): $\delta = 156.2$, 141.8, 129.3 (Py), 46.3 (P*C*), 31.8 ppm (PC*C*H$_3$); ^{31}P NMR ([D$_6$]acetone, 25°C) $\delta = 327.8$ (s), −140.8 ppm (sp, $^1J_{PF} = 708$ Hz, PF_6); $^{195}Pt\{^1H\}$ NMR ([D$_6$]acetone, 25°C): $\delta = -4343$ (2Pt), −3406 ppm (4Pt); IR (CH_2Cl_2): $\tilde{\nu} = 2031$ cm^{-1} (CO); el-

emental analysis calcd (%) for $C_{46}H_{82}F_{12}N_2O_4P_6Pt_6$: C 23.9, H 3.58; found: C 23.7, H 3.39.

Preparation of $[Pt_6(\mu\text{-}PtBu_2)_4(CO)_4(COOCH_3)_2]$ (13): A solution of CH_3OLi (100 μL, 0.15 mmol, 1.5 M) in methanol was added to a solution of complex **1**-Y_2 (45 mg, 0.0203 mmol) in acetone (4 mL). Complex **13** precipitated out quickly as an orange powder, which was isolated by filtration and then vacuum dried (34 mg, 85%). ^{1}H NMR (C_6D_6, 25°C) δ = 3.64[#] (s, $^4J_{HPt}$ = 7.5 Hz, 6H; OCH_3), 1.38 ppm (vt, ^3J(H,P)+^5J(H,P) = 7.5 Hz, 72H; PCCH_3); ^{13}C{^{1}H} NMR ($CDCl_3$, 25°C): δ = 218.8[#] (s, $^1J_{CPt}$ = 1529 Hz, *C*O), 201.5[#] (s, $^1J_{CPt}$ = 1486 Hz, *C*OOR), 48.9[#] (s, $^3J_{CPt}$ = 32 Hz, COO*C*H_3), 43.6 (s, PC), 31.4 ppm (s, PC*C*H_3); ^{31}P NMR (C_6D_6, 25°C) δ = 330.4[#] ppm (s); ^{195}Pt{^{1}H} NMR (C_6D_6, 25°C): δ = −4844 (2Pt), −2804 ppm (4Pt); IR (CaF_2, C_6D_6): $\tilde{\nu}$ = 2015 (C≡O), 1704 cm^{-1} (C=O); elemental analysis calcd (%) for $C_{40}H_{78}O_8P_4Pt_6$: C 24.2, H 3.97; found: C 24.6, H 4.03.

Preparation of $[Pt_6(\mu\text{-}PtBu_2)_4(CO)_4H_2]$ (14): $NaBH_4$ (10 mg, 0.264 mmol) was added to an orange solution of **3** (200 mg, 0.103 mmol) in THF (15 mL). After 12 h NaCl was filtered off and the solvent was evaporated. The red powder residue was suspended in acetone (5 mL), filtered and then vacuum dried (162 mg, 81%). ^{1}H NMR (C_6D_6, 25°C): δ = 1.41 (vt, $^3J_{HP}+^5J_{HP}$ = 7 Hz, CCH_3), 0.09[#] ppm(m, $^1J_{HPt}$=1385 Hz, PtH); ^{31}P{^{1}H} NMR (C_6D_6, 25°C): δ = 342.0[#] ppm (s); ^{195}Pt{^{1}H} NMR (C_6D_6, 25°C): δ = −5146 (m, 2Pt), −2822 ppm (m, 4Pt); IR (KBr, nujol): $\tilde{\nu}$ = 2001 (CO) cm^{-1}; elemental analysis calcd (%) for $C_{36}H_{74}O_4P_4Pt_6$: C 23.2, H 4.00; found: C 23.3, H 3.98.

Preparation of $[Pt_6(\mu\text{-}PtBu_2)_4(CNtBu)_6][CF_3SO_3]_2$ (15-Y_2): *tert*-Butyl isocyanide (68 μL, d = 0.735 g mL$^-$; 0.60 mmol) was added to an acetone solution (5 mL) of complex **1**-Y_2 (67 mg, 0.030 mmol). The solution quickly turned deep red and, after 12 H; the solvent was evaporated and the residue suspended in Et_2O (10 mL). A red powder was isolated by filtration and vacuum dried (57 mg, 75%). ^{1}H NMR ($CDCl_3$, 25°C) δ = 1.63 (s, 18H; 2CNCCH_3), 1.44 (vt, $^3J_{HP}+^5J_{HP}$ = 7 Hz, 72H; PCCH_3); 1.37 ppm (s, 36H; 4CNCCH_3); ^{13}C{^{1}H} NMR ($CDCl_3$, 25°C) δ = 166.9[#] (s, $^1J_{CPt}$ = 1570 Hz, 4*C*N), 135.2[#] (s, 2*C*N), 59.7 (s, 2CN−*C*), 59.2 (s, 4CN−*C*), 41.7 (s, P*C*), 32.8 (s, PC*C*H_3), 30.2 (s, 2CN−*CC*H_3), 30.1 ppm (s, 4CN−*CC*H_3); ^{31}P{^{1}H} NMR ($CDCl_3$, 25°C) δ = 300.5[#] ppm (s); ^{195}Pt{^{1}H} NMR ($CDCl_3$, 25°C) δ = −5130.7 (m, 2Pt), −3083.4 ppm (m, 4Pt); IR (CH_2Cl_2): $\tilde{\nu}$ = 2169 (CN), 2131 cm^{-1} (CN); elemental analysis calcd (%) for $C_{64}H_{126}F_6N_6O_6P_4Pt_6S_2$: C 30.2, H 4.98, N 3.30; found: C 30.0, H 4.78, N 3.22.

Preparation of $[Pt_6(\mu\text{-}PtBu_2)_4(CN\text{-}C_6H_4\text{–}4\text{-}C{\equiv}CH)_6][CF_3SO_3]_2$ (16-Y_2): CN-C_6H_4-4-C≡CH (152 mg, 1.20 mmol) was added to a chloroform solution (10 mL) of complex **1**-Y_2 (140 mg, 0.063 mmol). The solution quickly turned deep red and, after 12 H; the solvent was evaporated and the residue suspended in Et_2O (10 mL). A red powder was isolated by filtration and vacuum dried (142 mg, 80%). ^{1}H NMR ($CDCl_3$, 25°C) δ = 7.60 (d, $^3J_{HH}$ = 8 Hz, 4H; Ar*H*), 7.56 (d, $^3J_{HH}$ = 8 Hz, 8H; Ar*H*), 7.37 (d, $^3J_{HH}$ = 8 Hz, 4H; Ar*H*), 7.29 (d, $^3J_{HH}$ = 8 Hz, 8H; Ar*H*), 3.32 (s, 2H; C*CH*), 3.25 (s, 4H; C*CH*), 1.47 ppm (vt, $^3J_{HP}+^5J_{HP}$ = 7 Hz, 72H; PCCH_3); ^{13}C{^{1}H} NMR ($CDCl_3$, 25°C) δ = 178.4[#] (s, 4CN), 147.8[#] (s, 2CN), 134.0 (s, 4C), 133.9 (s, 8C), 128.4 (s, 4C), 127.6[#] (s, $^3J_{CPt}$ = 25 Hz, 2C), 126.2 (s, 8C), 125.2 (s, 4C), 124.7[#] (s, $^3J_{CPt}$ = 28 Hz, 4C), 123.6 (s, 2C), 82.2 (s, 2*C*CH), 82.0 (s, 4*C*C), 82.4 (s, 2*C*CH), 81.9 (s, 4*C*CH), 43.1 (s, PC), 31.7 ppm (s, PCCH$_3$); ^{31}P{^{1}H} NMR ([D$_6$]acetone, 25°C) δ = 323.4[#] ppm (s); ^{195}Pt{^{1}H} NMR ($CDCl_3$, 25°C) δ = −4980.7 (2Pt), −2995.7 ppm (4Pt); IR (CH_2Cl_2)$\tilde{\nu}$ = 3311 (CCH), 3294 (CCH), 2150 (CN), 2122 cm^{-1} (CN); elemental analysis calcd (%) for $C_{88}H_{102}F_6N_6O_6P_4Pt_6S_2$: C 37.6, H 3.66, N 2.99; found: C 38.0, H 3.78, N 3.02.

X-ray diffraction: The X-ray diffraction experiments were carried out at room temperature (T = 293 K) by means of a Bruker P4 diffractometer and a Bruker Apex II diffractometer, by operating with a graphite-monochromated $Mo_{K\alpha}$ radiation. The samples were sealed in glass capillaries under a dinitrogen atmosphere. The intensity data collection was carried out with the $\omega/2\theta$ scan mode, collecting a redundant set of data. Three standard reflections were measured every 97 measurements to check sample decay. The intensities were corrected for Lorentz and polarization effects and for absorption. In the case of **5** and **9**-Y_2·$CHCl_3$ the absorption correction was made by means of an integration method based on the crystal habit.[28] For **6**, the crystal fragment used in data collection was rather irregular, therefore a precise numerical correction was impossible and a semiempirical method was used.[28] An empirical method (SADABS)[29] was used for compound **3**. The structure solutions were obtained by means of the automatic direct methods contained in SHELXS97 program.[30] The refinement, based on full-matrix least-squares on F^2, were done by means of the SHELXL97[30] program. Some other utilities contained in the WINGX suite[31] were also used. The more relevant crystal parameters are listed in Table 5. The structure solution of compound **3** was found by automatic direct methods in the space group $I\bar{4}2d$. A molecule $[Pt_6(\mu\text{-}PtBu_2)_4(CO)_4Cl_2]$ is placed in the Wickoff site *b*, site symmetry $\bar{4}$. Hydrogen atoms were placed in calculated positions and let to ride on the connected carbon atoms. The reliability factors obtained after the last refinement cycle with anisotropic thermal pa-

Table 5. Crystal data and structure refinements

Compound	**3**	**5**	**6**	**9**-Y_2·$CHCl_3$
empirical formula	$C_{36}H_{72}Cl_2O_4P_4Pt_6$	$C_{36}H_{72}I_2O_4P_4Pt_6$	$C_{36}H_{72}ClIO_4P_4Pt_6$	$C_{45}H_{91}Cl_3F_6O_{10}P_6Pt_6S_2$
formula weight	1934.26	2117.16	2025.71	2432.97
crystal system	tetragonal	tetragonal	tetragonal	triclinic
space group	$I\bar{4}2d$ (No. 122)	$I4_1/amd$ (No. 141)	$I4_1/amd$ (No. 141)	$P\bar{1}$ (No. 2)
a [Å]	17.3763(5)	17.396(2)	17.487(1)	12.126(2)
b [Å]	17.3763(5)	17.396(2)	17.487(1)	14.667(3)
c [Å]	17.668(1)	17.698(4)	17.889(4)	21.099(4)
α [°]	–	–	–	93.06(2)
β [°]	–	–	–	92.76(1)
γ [°]	–	–	–	105.83(1)
U [Å^3]	5334.7(4)	5355.8(15)	5470.4(13)	3597.2(10)
Z	4	4	4	2
ρ_{calc} [g cm^{-3}]	2.408	2.626	2.460	2.246
μ [mm^{-1}]	15.925	16.915	16.045	11.985
reflns measured	29939	2997	3206	10364
reflns unique [R_{int}]	3316 [0.0341]	1267 [0.0561]	1372 [0.0463]	8845 [0.0357]
no. parameters	125	54	71	638
R_1, wR_2 [$I > 2\sigma(I)$][a]	0.0172, 0.0472	0.0478, 0.0867	0.0398, 0.0942	0.0353, 0.1024
R_1, wR_2 [all data][a]	0.0182, 0.0474	0.0670, 0.0917	0. 0.0639, 0.1009	0.0531, 0.1069
goodness of fit[a] on F^2	1.209	1.188	1.166	0.952

[a] $R(F_o) = \Sigma||F_o| - |F_c||\Sigma|F_o|$; $Rw(F_o^2) = [\Sigma[w(F_o^2 - F_c^2)^2]/\Sigma[w(F_o^2)^2]]^{1/2}$; $w = 1/[\sigma^2(F_o^2) + (AQ)^2 + BQ]$, where $Q = [MAX(F_o^2,0) + 2F_c^2]/3$; GOF = $[\Sigma[w(F_o^2 - F_c^2)^2]/(N-P)]^{1/2}$, where N, P are the numbers of observations and parameters, respectively.

rameters for all the non-hydrogen atoms are listed in Table 5. The structure solution of compound **5** indicated a molecule $[Pt_6(\mu\text{-}PtBu_2)_4(CO)_4I_2]$ placed in the Wickoff site *a*, site symmetry $\bar{4}m2$. The Pt and P atoms and the CO groups lie on the mirrors and the I atoms are placed along the $\bar{4}$ axis. The *t*-butyl groups of the phosphido moieties are disordered and were refined as distributed on two limit positions distinguished by different rotations around the P–C bond and by different occupancy factors. The total occupancy for the corresponding atoms of the disordered group was fixed to 1.0. The reliability factors obtained after the last refinement cycle with anisotropic thermal parameters for ordered atoms and isotropic for the other ones are listed in Table 5. Both the lattice parameters and the intensity data layout suggested the structure of $[Pt_6(\mu\text{-}PtBu_2)_4(CO)_4ICl]$ was isotypical with that of $[Pt_6(\mu\text{-}PtBu_2)_4(CO)_4I_2]$. Since the former cannot posses the symmetry $\bar{4}m2$ for the evident absence of the twofold axes, it can adopt this structure only in the presence of disorder in the molecule orientation. So we started the structure analysis by refining the two independent platinum atoms, the phosphido and the carbonyl positions kept from the structure of $[Pt_6(\mu\text{-}PtBu_2)_4(CO)_4I_2]$. The following difference Fourier map showed two maxima partially superimposed, owing to one half of iodine and one half of chlorine atoms statistically connected to the same Pt(2) atom. The iodine and chlorine atoms were introduced in calculations with an occupancy factor equal to 1/8 with the only constraint of remaining on the $\bar{4}$ axis. The model containing 71 parameters refined till a final *R* factor of 0.0398. In order to exclude the possibility that the correspondence of the space groups of the structures of compounds **5** and **6** was an artifact as a result of the predominance of the platinum contribution to the structure factors, we tried to refine the structure of $[Pt_6(\mu\text{-}PtBu_2)_4(CO)_4ICl]$ in the space group *I*4*md* (No. 109), which in the Wyckoff position *a* shows a symmetry 2*mm*, thus allowing the use of an ordered model with iodine at one side of the metal cluster and the chlorine to the other. This model, however, notwithstanding the use of an almost double number of parameters, refined to a significantly higher *R* factor (0.070). So the disordered model in the higher symmetry space group was assumed as correct. The crystal of $[Pt_6(\mu\text{-}PtBu_2)_4(CO)_4(PMe_3)_2][CF_3SO_3]_2$ showed triclinic symmetry with the lattice parameters listed in Table 5. The structure solution was obtained in the $P\bar{1}$ space group with automatic statistical methods. Together with the ionic moieties of the substance, one molecule of chloroform, used as crystallization solvent, was also found in the asymmetric unit. The final refinement cycle with hydrogen atoms in calculated positions and all the non hydrogen atoms with anisotropic thermal parameters gave the reliability factors listed in Table 5. CCDC 647407–647410 contain the supplementary crystallographic data for this paper. These data can be obtained free of charge from The Cambridge Crystallographic Data Centre via www.ccdc.cam.ac.uk/data_request/cif.

Acknowledgements

This work was supported by the Ministero dell′Istruzione, dell′Universita′ e della Ricerca (MIUR), Programmi di Rilevante Interesse Nazionale, PRIN 2006–2007. Dr. Stefano Zacchini, Bologna University, is gratefully acknowledged for the collection of diffraction data of compound **3**.

[1] a) M.-S. Choi, T. Yamazaki, I. Yamazaki, T. Aida, *Angew. Chem.* **2003**, *116*, 152; *Angew. Chem. Int. Ed.* **2003**, *43*, 150; b) F. Hof, S. L. Craig, C. Nuckolls, J. Rebeck Jr. , *Angew. Chem.* **2002**, *114*, 1556; *Angew. Chem. Int. Ed.* **2002**, *41*, 1488; c) S. R. Seidel, P. J. Stang, *Acc. Chem. Res.* **2002**, *35*, 972; d) G. F. Swiegers, T. J. Malefetse, *Chem. Rev.* **2000**, *100*, 3483; e) A. Müller, P. Kögerler, *Coord. Chem. Rev.* **1999**, *182*, 3; f) P. F. H. Schwab, M. D. Levin, J. Michl, *Chem. Rev.* **1999**, *99*, 1863; g) G. R. Newkome, E. He, C. N. Moorefield, *Chem. Rev.* **1999**, *99*, 1689.

[2] a) N. Robertson, C. A. McGowan, *Chem. Soc. Rev.* **2003**, *32*, 96; b) C. Janiak, *Dalton Trans.* **2003**, 2781; c) M. C. Jimenez-Molero, C. Dietrich-Buchecker, J.-P. Sauvage, *Chem. Commun.* **2003**, 1613; d) molecular machines special issue *Acc. Chem. Res.* **2001**, *34*, 409; e) B. J. Holliday, C. A. Mirkin, *Angew. Chem.* **2001**, *113*, 2076; *Angew. Chem. Int. Ed.* **2001**, *40*, 2022; f) D. Gust, T. A. Moore, A. L. Moore, *Acc. Chem. Res.* **2001**, *34*, 40; g) V. Balzani, A. Credi, F. M. Raymo, J. F. Stoddart, *Angew. Chem.* **2000**, *112*, 3484; *Angew. Chem. Int. Ed.* **2000**, *39*, 3349.

[3] a) S. Szafert, J. A. Gladysz, *Chem. Rev.* **2003**, *103*, 4175; b) T. L. Stott, M. O. Wolf, *Coord. Chem. Rev.* **2003**, *246*, 89; c) F. Paul, C. Lapinte, *Coord. Chem. Rev.* **1998**, *178–180*, 431.

[4] a) G.-L. Xu, G. Zou, Y.-H. Ni, M. C. DeRosa, R. J. Crutchley, T. Ren, *J. Am. Chem. Soc.* **2003**, *125*, 10057; b) F. A. Cotton, C. Lin, C. A. Murillo, *Acc. Chem. Res.* **2001**, *34*, 759; c) M. H. Chisholm, *Acc. Chem. Res.* **2000**, *33*, 53; d) K.-T. Wong, J.-M. Lehn, S.-M. Peng, G.-H. Lee, *Chem. Commun.* **2000**, 2259; e) M. J. Irwin, G. Jia, J. J. Vittal, R. J. Puddephatt, *Organometallics* **1996**, *15*, 5321.

[5] a) T.-B. Tsao, G.-H. Lee, C.-Y. Yeh, S.-M. Peng, *Dalton Trans.* **2003**, 1465; b) J. F. Berry, F. A. Cotton, C. A. Murillo, *Dalton Trans.* **2003**, 3015; c) J. K. Bera, K. R. Dunbar, *Angew. Chem.* **2002**, *114*, 4633; *Angew. Chem. Int. Ed.* **2002**, *41*, 4453.

[6] a) D. Kim, A. Osuka, *J. Phys. Chem. A* **2003**, *107*, 8791; b) D. Holten, D. F. Bocian, J. S. Lindsey, *Acc. Chem. Res.* **2002**, *35*, 57; c) H. E. Toma, K. Araki, *Coord. Chem. Rev.* **2000**, *196*, 307.

[7] a) Z. Peng, *Angew. Chem.* **2004**, *116*, 948; *Angew. Chem. Int. Ed.* **2004**, *43*, 930; b) H. Zeng, G. R. Newkome, C. L. Hill, *Angew. Chem.* **2000**, *112*, 1841; *Angew. Chem. Int. Ed.* **2000**, *39*, 1772; c) P. G. Hagrman, D. Hagrman, J. Zubieta, *Angew. Chem.* **1999**, *111*, 2798; *Angew. Chem. Int. Ed.* **1999**, *38*, 2638.

[8] a) T. J. Wedge, A. Herzog, R. Huertas, M. W. Lee, C. B. Knobler, M. F. Hawthorne, *Organometallics* **2004**, *23*, 482; b) J. Vicente, M.-T. Chicote, M. M. Alvarez-Falcón, M. A. Fox, D. Bautista, *Organometallics* **2003**, *22*, 4792; c) H. Yao, M. Sabat, R. N. Grimes, F. Fabrizi de Biani, P. Zanello, *Angew. Chem.* **2003**, *115*, 1032; *Angew. Chem. Int. Ed.* **2003**, *42*, 1002; d) M. A. Fox, M. A. J. Paterson, C. Nervi, F. Galeotti, H. Puschmann, J. A. K. Howard, P. J. Low, *Chem. Commun.* **2001**, 1610; e) A. S. Batsanov, M. A. Fox, J. A. K. Howard, J. A. H. Mac Bride, K. Wade, *J. Organomet. Chem.* **2000**, *610*, 20; f) C. Mazal, A. J. Paraskos, J. Michl, *J. Org. Chem.* **1998**, *63*, 2116; g) W. Jiang, D. E. Harwell, M. D. Mortimer, C. B. Knobler, M. F. Hawthorne, *Inorg. Chem.* **1996**, *35*, 4355.

[9] K. Lee, H. Song, J. T. Park, *Acc. Chem. Res.* **2003**, *36*, 78.

[10] H.-F. Chow, C.-F. Leung, W. Li, K.-W. Wong, L. Xi, *Angew. Chem.* **2003**, *115*, 5069; *Angew. Chem. Int. Ed.* **2003**, *42*, 4919.

[11] P. Zanello, F. Fabrizi de Biani in *Metal Clusters in Chemistry* (Eds.: P. Braunstein, L. A. Oro, P. R. Raithby), Wiley-VCH, Weinheim, **1999**; Vol. 2, p. 1104.

[12] a) A. Choualeb, P. Braunstein, J. Rosé, R. Welter, *Inorg. Chem.* **2004**, *43*, 57; b) B. K. Roland, H. D. Selby, J. R. Cole, Z. Zheng, *Dalton Trans.* **2003**, 4307; c) M. Akita, A. Sakurai, M.-C. Chung, Y. Moro-oka, *J. Organomet. Chem.* **2003**, *670*, 2; d) B.-H. Zhu, B. Hu, W.-Q. Zhang, Y.-H. Zhang, Y.-Q. Yin, J. Sun, *J. Organomet. Chem.* **2003**, *681*, 275; e) M. I. Bruce, M. E. Smith, N. N. Zaitseva, B. W. Skelton, A. H. White, *J. Organomet. Chem.* **2003**, *670*, 170; f) M. D. Westmeyer, M. A. Massa, T. B. Rauchfuss, S. R. Wilson, *J. Am. Chem. Soc.* **1998**, *120*, 114; g) J. W.-S. Hui, W.-T. Wong, *J. Chem. Soc. Dalton Trans.* **1997**, 2445; h) D. Imhof, U. Burkhardt, K.-H. Dahmen, F. Joho, R. Nesper, *Inorg. Chem.* **1997**, *36*, 1813; i) V. W.-W. Yam, W. K.-M. Fung, K.-K. Cheung, *Chem. Commun.* **1997**, 963; j) D. Osella, L. Milone, C. Nervi, M. Ravera, *J. Organomet. Chem.* **1995**, *488*, 1; k) M. P. Jensen, D. A. Phillips, M. Sabat, D. F. Shriver, *Organometallics* **1992**, *11*, 1859; l) G. H. Worth, B. H. Robinson, *Organometallics* **1992**, *11*, 501; m) F. R. Furuya, L. L. Miller, J. F. Hainfeld, W. C. Christopfel, P. W. Kenny, *J. Am. Chem. Soc.* **1988**, *110*, 641.

[13] a) E. G. A. Notaras, N. T. Lucas, M. G. Humphrey, A. C. Willis, A. D. Rae, *Organometallics* **2003**, *22*, 3659; b) B. K. Roland, C. Carter, Z. Zheng, *J. Am. Chem. Soc.* **2002**, *124*, 6234; c) N. Feeder, J. Geng, P. G. Goh, B. F. G. Johnson, C. M. Martin, D. S. Shepard, W. Zhou, *Angew. Chem.* **2000**, *112*, 1727; *Ang. Chem. Int. Ed.* **2000**, *39*, 1661; d) E. Alonso, D. Astruc, *J. Am. Chem. Soc.* **2000**, *122*, 3222; e) M. Benito, O. Rossell, M. Seco, G. Segalés, *Organometallics* **1999**,

18, 5191; f) X. Lei, E. E. Wolf, T. P. Fehlner, *Eur. J. Inorg. Chem.* **1998**, 1835; g) U. Ritter, N. Winkhofer, R. Murugavel, A. Voigt, D. Stalke, H. W. Roesky, *J. Am. Chem. Soc.* **1996**, *118*, 8580.

[14] a) A. Albinati, P. Leoni, L. Marchetti, S. Rizzato, *Angew. Chem.* **2003**, *115*, 6172; *Angew. Chem. Int. Ed.* **2003**, *42*, 5990; b) P. Leoni, F. Marchetti, L. Marchetti, M. Pasquali, *Chem. Commun.* **2003**, 2372; c) P. Leoni, L. Marchetti, S. K. Mohapatra, G. Ruggeri, L. Ricci, *Organometallics* **2006**, *25*, 4226; d) A. Albinati, F. Fabrizi de Biani, P. Leoni, L. Marchetti, M. Pasquali, S. Rizzato, P. Zanello, *Angew. Chem.* **2005**, *117*, 5847; *Angew. Chem. Int. Ed.* **2005**, *44*, 5701.

[15] The structures cited in ref. [12–14] generally contain low valent carbonyl clusters. Related works describe the preparation of polymers or extended 3-D coordination or hydrogen-bonded networks, mainly constructed with medium-valent halide or calchogenide clusters: a) B. K. Roland, H. D. Selby, J. R. Cole, Z. Zheng, *Dalton Trans.* **2003**, 4307; b) B. Yan, H. Zhou, A. Lachgar, *Inorg. Chem.* **2003**, *42*, 8818; c) C. W. Liu, C.-M. Hung, H.-C. Haia, B.-J. Liaw, L.-S. Liou, Y.-F. Tsai, J.-C. Wang, *Chem. Commun.* **2003**, 976; d) S. Cordier, F. Gulo, T. Roisnel, R. Gautier, B. le Guennic, J. F. Halet, C. Perrin, *Inorg. Chem.* **2003**, *42*, 8320; e) S. Jin, F. J. DiSalvo, *Chem. Mater.* **2002**, *14*, 3448; f) M. V. Bennett, L. G. Beauvais, M. P. Shores, J. R. Long, *J. Am. Chem. Soc.* **2001**, *123*, 8022; g) Y. Kim, S.-M. Park, W. Nam, S.-J. Kim, *Chem. Commun.* **2001**, 1470; h) T. Nakajima, A. Ishiguro, Y. Wakatsuki, *Angew. Chem.* **2001**, *113*, 1096; *Angew. Chem. Int. Ed.* **2001**, *40*, 1066; i) N. Prokopuk, C. S. Weinert, D. P. Siska, C. L. Stern, D. F. Shriver, *Angew. Chem.* **2000**, *112*, 3450; *Angew. Chem. Int. Ed.* **2000**, *39*, 3312; j) N. G. Naumov, A. V. Virovets, M. N. Sokolov, S. B. Artemkina, V. E. Fedorov, *Angew. Chem.* **1998**, *110*, 2043; *Angew. Chem. Int. Ed.* **1998**, *37*, 1943; k) A. M. Bradford, E. Kristof, M. Rashidi, D.-S. Yang, N. C. Payne, R. J. Puddephatt, *Inorg. Chem.* **1994**, *33*, 2355.

[16] P. Leoni, F. Marchetti, L. Marchetti, M. Pasquali, S. Quaglierini, *Angew. Chem.* **2001**, *113*, 3729; *Angew. Chem. Int. Ed.* **2001**, *40*, 3617.

[17] a) D. Braga, F. Grepioni, M. D. Vargas, C. M. Ziglio, *J. Braz. Chem. Soc.* **2002**, *13* 682; b) A. Fumagalli, S. Martinengo, G. Bernasconi, L. Noziglia, V. G. Albano, M. Monari, C. Castellari, *Organometallics* **2000**, *19*, 5149; c) R. Vilar, S. E. Lawrence, S. Menzer, D. M. P. Mingos, D. J. Williams, *J. Chem. Soc. Dalton Trans.* **1997**, 3305; d) M. Breuer, J. Strähle, *Z. Anorg. Allg. Chem.* **1993**, *619*, 1564; e) U. Florke, H.-J. Haupt, *Z. Kristallogr.* **1990**, *193*, 309; f) E. G. Mednikov, N. K. Eremenko, Yu. L. Slovokhotov, Yu. T. Struchkov, *Metalloorg. Khim.* **1989**, *2*, 1289; g) G. Ciani, G. D′Alfonso, P. Romiti, A. Sironi, M. Freni, *Inorg. Chem.* **1983**, *22*, 3115; h) R. J. Haines, N. D. C. T. Steen, R. B. English, *J. Chem. Soc. Dalton Trans.* **1983**, 2229; i) Z. Beni, R. Ros, A. Tassan, R. Scopelliti, R. Roulet, *Dalton Trans.* **2005**, 315; j) R. S. Dickson, G. D. Fallon, M. J. Liddel, B. W. Skelton, A. H. White, *J. Organomet. Chem.* **1987**, *327*, C51; k) C. G. Arena, F. Faraone, M. Lanfranchi, E. Rotondo, A. Tiripicchio, *Inorg. Chem.* **1992**, *31*, 4797; l) J. W.-S. Hui, W.-T. Wong, *J. Cluster Sci.* **1999**, *10*, 91.

[18] F. H. Allen, *Acta Crystallogr. Sect. B* **2002**, *58*, 380–388.

[19] The ^{1}H NMR spectra of **3**–**5** contain only the resonances due to the *t*-butyl protons, they appear, as for **1**-Y_2, as virtual triplets at $\approx$1.5 ppm ($^3J_{HP}+{}^5J_{HP}=\approx$7 Hz), again confirming that the structure of the $Pt_6(\mu\text{-}P)_4(CO)_4$ core remains nearly unchanged.

[20] a) B. E. Mann, C. Masters, B. L. Shaw, *J. Chem. Soc. Dalton Trans.* **1972**, 704; b) P. E. Garrou, G. E. Hartwell, *Inorg. Chem.* **1976**, *15*, 646; c) E. M. Hyde, J. D. Kennedy, B. L. Shaw, W. McFarlane, *J. Chem. Soc. Dalton Trans.* **1977**, 1571; d) J. J. Mac Dougall, J. H. Nelson, F. Mathey, *Inorg. Chem.* **1982**, *21*, 2145; e) J. A. Rahn, D. J. O'Donnell, A. R. Palmer, J. H. Nelson, *Inorg. Chem.* **1989**, *28*, 2631; f) S. O. Grim, P. J. Lui, R. L. Keiter, *Inorg. Chem.* **1974**, *13*, 342; g) E. C. Alyea, S. A. Dias, R. G. Goel, W. O. Ogini, P. Pilon, D. W. Meek, *Inorg. Chem.* **1978**, *17*, 1697.

[21] Selected examples in: a) M. Ebihara, M. Iiba, H. Matsuoka, T. Kawamura, *Inorg. Chim. Acta* **2004**, *357*, 1236; b) S. Y.-W. Hung, W.-T. Wong, *Chem. Commun.* **1997**, 2099; c) E. Simon-Manso, C. P. Kubiak, *Angew. Chem.* **2005**, *117*, 1149; *Angew. Chem. Int. Ed.* **2005**, *44*, 1125; d) R. Vilar, S. E. Lawrence, S. Menzer, D. M. P. Mingos, D. J. Williams, *J. Chem. Soc. Dalton Trans.* **1997**, 3305; e) M. J. A. Johnson, P. K. Gantzel, C. P. Kubiak, *Organometallics* **2002**, *21*, 3831; f) T. Zhang, M. Drouin, P. D. Harvey, *Chem. Commun.* **1996**, 877; g) D. M. P. Mingos, R. W. M. Wardle, *J. Chem. Soc. Dalton Trans.* **1986**, 73; h) D. M. P. Mingos, P. Oster, D. J. Sherman, *J. Organomet. Chem.* **1987**, *320*, 257; i) W. Schuh, H. Wachtler, G. Laschober, H. Kopacka, K. Wurst, P. Peringer, *Chem. Commun.* **2000**, 1181; j) J. Xiao, L. Hao, R. J. Puddephatt, L. Manojlovic-Muir, K. W. Muir, A. A. Torabi, *Organometallics* **1995**, *14*, 2194.

[22] Selected examples in: a) X. Fan, R. Cao, M. Hong, W. Su, D. Sun, *J. Chem. Soc. Dalton Trans.* **2001**, 2961; b) D. Fenske, H. Fleischer, H. Krautscheid, J. Magull, C. Oliver, S. Weisgerber, *Z. Naturforsch. B: Chem. Sci.* **1991**, *46*, 1384; c) S. Koenig, D. Fenske, *Z. Anorg. Allg. Chem.* **2004**, *630*, 2720.

[23] a) D. G. Holah, A. N. Hughes, E. Krysa, G. J. Spivak, M. D. Havighurst, V. R. Magnuson, *Polyhedron* **1997**, *16*, 2353; b) K. Matsumoto, S. Arai, M. Ochiai, W. Chen, A. Nakata, H. Nakai, S. Kinoshita, *Inorg. Chem.* **2005**, *44*, 8552; c) K. Sakai, Y. Tanaka, Y. Tsuchiya, K. Hirata, T. Tsubomura, S. Iijima, A. Bhattacharjee, *J. Am. Chem. Soc.* **1998**, *120*, 8366; d) A. Poater, S. Moradell, E. Pinilla, J. Poater, M. Sola, M. A. Martinez, A. Llobet, *Dalton Trans.* **2006**, 1188; e) F. Liu, W. Chen, D. Wang, *Dalton Trans.* **2006**, 3445.

[24] a) Z. Beni, R. Ros, A. Tassan, R. Scopelliti, R. Roulet, *Dalton Trans.* **2005**, 315; b) C. Archambault, R. Bender, P. Braunstein, S.-E. Bouaoud, D. Rouag, S. Golhen, L. Ouahab, *Chem. Commun.* **2001**, 849; c) W. Schuh, H. Wachtler, G. Laschober, H. Kopacka, K. Wurst, P. Peringer, *Chem. Commun.* **2000**, 1181.

[25] F. Fabrizi de Biani, A. Ienco, F. Laschi, P. Leoni, F. Marchetti, L. Marchetti, C. Mealli, P. Zanello, *J. Am. Chem. Soc.* **2005**, *127*, 3076.

[26] a) Actually, in spite of the apparent chemical reversibility of the two first one-electron additions, exhaustive electrolysis causes the formation of minor by-products, identified as the mono- or dichloride derivatives **2**-Y and **3** (ref. [25]). b) Exhaustive electrolysis of **3**–**6** leads to minor unidentified by-products if performed in correspondence of the first reduction, whereas **2**-Y tends to slowly generate complex **3** in correspondence of the first reduction.

[27] P.Zanello, *Inorganic electrochemistry. Theory, practice and application*, RSC, Oxford, **2003**.

[28] G. M. Sheldrick, *SHELXTL-Plus*, *Rel. 5.1*, Bruker AXS Inc., Madison, Wisconsin, USA, **1997**.

[29] G. M. Sheldrick *SADABS*, Program for empirical absorption correction, University of Göttingen, Germany, **1996**.

[30] G. M. Sheldrick, *SHELX97*, *Programs for Crystal Structure Analysis*, (Release 97–2), University of Göttingen, Göttingen, Germany, **1998**.

[31] L. J. Farrugia, *J. Appl. Crystallogr.* **1999**, *32*, 837.

Received: May 21, 2007
Published online: September 28, 2007

